ChemPubSoc Europe

DOI: 10.1002/chem.201801416

CHEMISTRY A European Journal Full Paper

Metal–Organic Frameworks

Compartmentalization of Incompatible Polymers within Metal–Organic Frameworks towards Homogenization of Heterogeneous Hybrid Catalysts for Tandem Reactions

Jin-Hao Zhao,[b] Yong Yang,[a, b] Jin-Xin Che,[a] Jun Zuo,[b] Xiao-Hua Li,[c] Yong-Zhou Hu,[a] Xiao-Wu Dong,*[a] Liang Gao,*[d] and Xin-Yuan Liu*[c]

Abstract: New catalytic systems that contain incompatible catalytic sites were constructed by the in situ polymerization of acidic and basic polymers into metal–organic frameworks, which resulted in highly porous, recyclable, and durable catalytic composites with excellent compartmentalization, so that opposing agents were spatially isolated. These synthesized hybrid catalysts exhibited excellent catalytic activity for one-pot "wolf and lamb" reactions (deacetalization/Knoevenagel or Henry), which was attributed to their unique characteristic of having a locally homogeneous, but globally heterogeneous, structure.

Introduction

Enzymatic catalysis is one of the most advanced synthetic processes.[1] In addition to adaptive properties, enzymatic catalysis combines multiple incompatible catalytic sites that can effectively catalyze tandem reactions. The cascade process demonstrates superior performance to that of a conventional two-step reaction. The development of catalysts that can act like enzymes has attracted intense attention;[2] however, progress has been slow, because in conventional catalytic systems, these incompatible catalysts can be quenched or deactivated during the reaction. The trade-off between isolation of the active site and preservation of activity is still a challenging issue.

The concept of "wolf and lamb" reactions emerged as a powerful tool to probe site-isolation effects.[3] To catalyze a "wolf and lamb" reaction, the incompatible active sites are separately embedded into different heterogeneous solid supports, such as resin,[4] sol-gel colloids,[5] Pickering emulsions,[6] and polymeric micelles.[7] In general, the existing catalytic strategies that involve solid supports can be classified into two types: 1) Anchorage/encapsulation of the catalytic groups with opposite properties onto insoluble solids to form a heterogeneous catalyst; with this technique, the active sites, which can react with each other in solution, can be physically separated.[4,5] 2) Fabrication of soluble core-confined star/bottlebrush polymers, in which the incompatible reactive agents are located in the core and are sterically isolated from each other by long hydrophobic brush-like branches.[6,7] The first strategy benefits from relatively easy separation of the catalyst from the products and solution; however, the heterogeneous catalysts typically suffer from insufficient contact with the organic reactants. The second strategy has afforded homogeneous multifunctional catalysts with high levels of activity, but whose recyclability is still a challenge. Therefore, a mechanistically distinct strategy needs to be developed for the rational design of multifunctional catalysts for cascade reactions.

Metal–organic frameworks (MOFs) have become particularly attractive for a wide range of applications, such as gas storage,[8a,b] separation,[8c] drug delivery,[8d] and catalysis.[8e–g] Recently, Kitagawa, Uemura, and co-workers reported a series of MOF/polymer composites,[9] which provide a powerful tool for the integration of functional polymers and MOFs.[10] This new class of porous composite has the linear polymer threaded throughout the nanospace of the MOF. In principle, although there may exist strong interactions between the pore wall of the MOF and the polymer (e.g., hydrophobic and electrostatic interactions), the solvent can significantly reduce net segment–segment forces (e.g., electrostatic and van der Waals forces). Therefore, when it is in contact with the appropriate solvents, the polymer in the polymer/MOF composite can

[a] Y. Yang, J.-X. Che, Prof. Dr. Y.-Z. Hu, Dr. X.-W. Dong
College of Pharmaceutical Sciences, Zhejiang University
Hangzhou, 310058 (P.R. China)
E-mail: dongxw@zju.edu.cn

[b] Dr. J.-H. Zhao, Y. Yang, J. Zuo
Institute of Pesticide and Environmental Toxicology
Zhejiang University, Hangzhou, 310029 (P.R. China)

[c] Dr. X.-H. Li, Prof. Dr. X.-Y. Liu
Department of Chemistry, Shenzhen Grubbs Institute,
South University of Science and Technology of China
Shenzhen, 518055 (P.R. China)
E-mail: liuxy3@sustc.edu.cn

[d] Dr. L. Gao
School of Chemical Engineering and Light Industry
Guangdong University of Technology
Guangzhou, 510006 (P.R. China)
E-mail: gaoliang@gdut.edu.cn

Supporting information and the ORCID number(s) for the author(s) of this article can be found under https://doi.org/10.1002/chem.201801416.

detach from the wall of the MOF to reside in the MOF channel in accordance with the confinement effect, and the skeleton of the MOFs remains unchanged. In this sense, the composite has the characteristics of a locally homogeneous, but globally heterogeneous, structure. These features make polymer/MOF composites an ideal support to demonstrate the concept of a "wolf and lamb" reaction.

In juxtaposition to the abovementioned strategies, the use of polymer/MOF composites can combine heterogenous and homogenous properties in one single catalytic system to exploit their respective advantages whilst effectively avoiding their shortcomings. Herein, we have developed a novel "site-isolation" methodology by performing the convenient in situ polymerization of hostile vinyl substrates within MOFs to compartmentalize incompatible polymers (Figure 1). The excellent catalytic performance of the so-prepared MOF/polymer composites was demonstrated in a sequential two-step reaction.

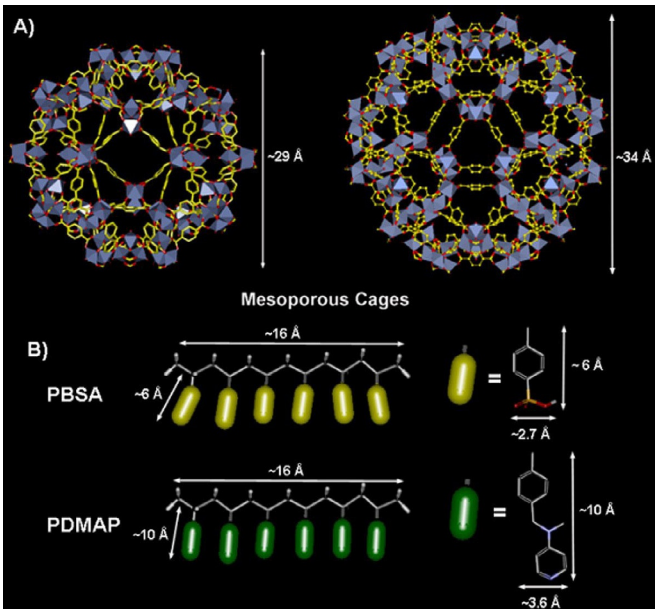

Figure 2. The topological characteristics of a) Cr-MIL-101 and (b) the proposed model for encapsulated linear polymer PBSA and PMAP (six repetitive units).

Results and Discussion

To validate the feasibility of the proposed "site-isolation" strategy, we selected the Cr-MIL-101 as a host material owing to its interconnected cage-type pore, its sufficiently large pore size to allow monomer penetration (Figure 2), and its reasonable stability against common solvents.[11,12] Benzene sulfonic acid (BSA) and methylaminopyridine (MAP) were chosen as agents to offer incompatible active sites.[4f,7c] The preparation of the acidic PBSA/MIL-101 and basic PMAP/MIL-101 was accomplished in two steps through the in situ polymerization strategy: 1) a solution of BSA- or MAP-containing vinyl derivative **S1** (see the Supporting Information) and 2,2-azobisisobutyronitrile (AIBN) in DMF/H_2O was impregnated into the porous cavities of Cr-MIL-101; 2) in situ radical polymerization of the preloaded vinyl compounds was initiated by heating. Upon sufficient contact, the monomer-containing solution was expected to penetrate into Cr-MIL-101, considering that the internal surface area of MIL-101 should be much larger than external one. Such kind of penetration can be simply driven by the favorable interaction between MIL-101 and polar DMSO solvent.[13] Although external surface adsorption of monomer also inevitably occurs, the amount should be much less than that of internal surface adsorption. When polymerization occurred, the monomer units in different cages polymerized through neighboring cavities, so that the formed polymer was physically interlocked inside the MOF. In situ polymerization was conducted to encapsulate BSA- or MAP-containing vinyl monomers into polystyrene, which led to the formation of the desired MOF/acidic/

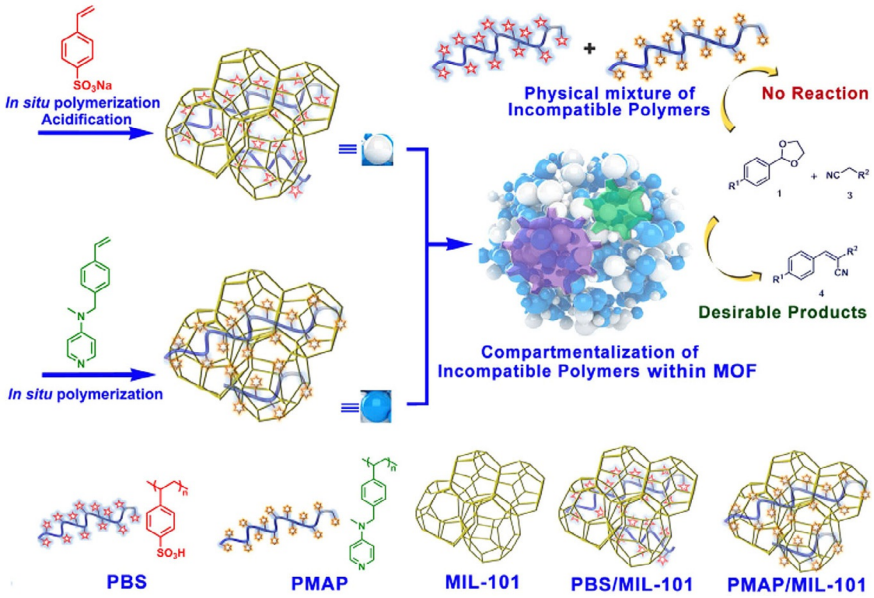

Figure 1. Compartmentalization of incompatible polymers within MOFs by in situ polymerization of hostile vinyl substrates for a tandem reaction.

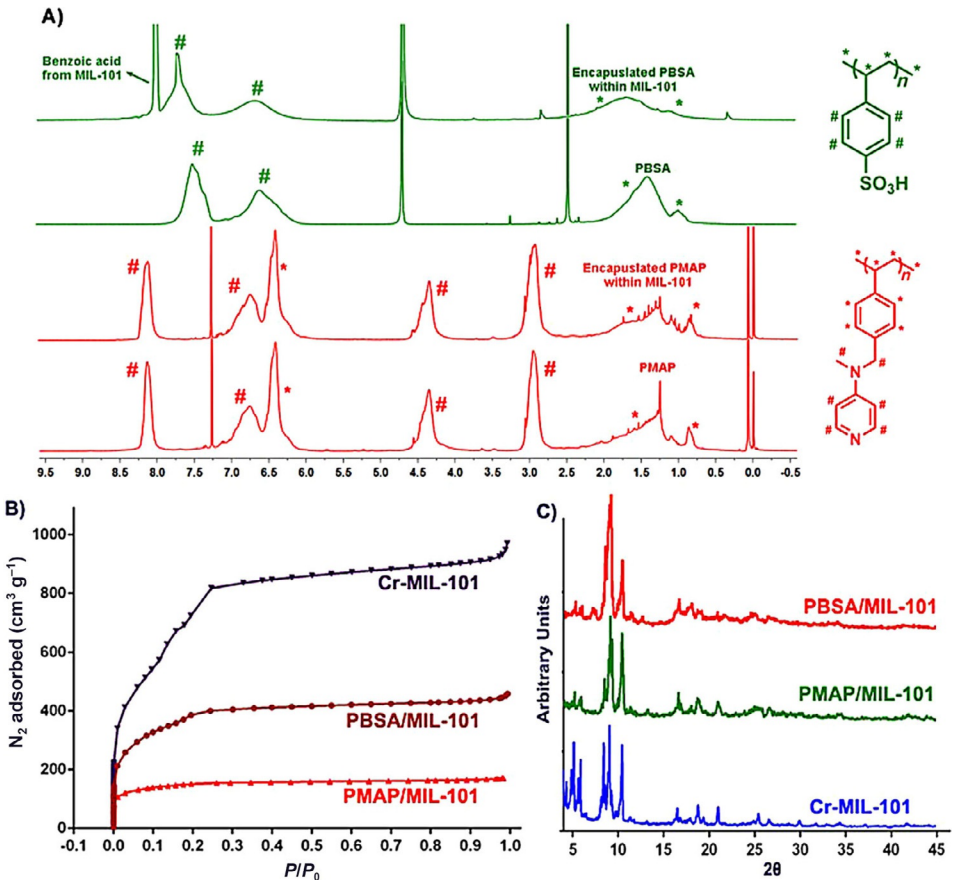

Figure 3. a) ^{1}H NMR spectra of encapsulated polymers of the digested PBSA/MIL-101, PMAP/MIL-101, and the bulk PP1 ([D_4]MeOH) prepared by a solution approach; b) N_2 isotherms for Cr-MIL-101, PBSA/MIL-101, and PMAP/MIL-101; c) PXRD measurements of Cr-MIL-101, PBSA/MIL-101, and PMAP/MIL-101.

basic polymer (Figure 1). The resultant polymeric chains were isolated by ordered pores of the MOF.

To confirm the polymeric and chemical structure of the polymer inside the MOF, the linear polymers (PBSA and PMAP) within the cavities of PBSA/MIL-101 and PMAP/MIL-101 were released and collected by digesting MIL-101 with a strong alkali. As shown in Figure 3a, proton chemical shifts in the NMR spectra match those of bulk PBSA and PMAP that had been prepared by using a solution-based approach (for the preparative protocol, see the Supporting Information). The broad peaks around $\delta = 7.5$ ppm belong to the aromatic protons of BSA, whereas the signals at $\delta = 2.96$, 4.40, 6.50, 6.80, and 8.10 ppm in the spectrum of PMAP/MIL-101 were assigned to the *N*-methyl group of the pyridine unit, benzyl hydrogen protons, and aromatic protons of the polymeric styrene and pyridine, respectively. Furthermore, the released PBSA and PMAP polymers were characterized by gel permeation chromatography (GPC) to have a number average molecular weight (Mn) of about 3600 and 7000, respectively (see the Supporting Information, Figure S1). This is equivalent to about 27 and 34 repeat units of PBSA and PMAP, the length of which is enough to intertwine within the cavities of Cr-MIL-101. The existence of acidic and basic active sites was also confirmed by using solid-state Fourier transform infrared spectroscopy (FTIR). In the FTIR spectra of polymer/MOF composites, characteristic bonds (e.g., S–O and C=N) of the incorporated polymers were observed (see the Supporting Information, Figure S2). These NMR and FTIR results demonstrated the successful anchorage of BSA and MAP onto the MOF during in situ polymerization. Then, the loaded amounts of polymers were quantified, which showed that there were 1.01 and 0.34 mmol of acidic and basic groups per gram of PBSA/MIL-101 and PMAP/MIL-101, respectively [see the Experimental Section, Eq. (1) and (2)]. Examination of the gas adsorption behavior indicated that all of the functionalized MOFs are porous (Figure 2b, Table 1). Their surface areas are still very large to ensure good contact with

Table 1. Textural structure and amount of active site of MOF and its composites.

Sample	BET surface area [$m^3 g^{-1}$]	Pore size[a] [nm]	Pore volume[b] [$mL g^{-1}$]	Amount of active site[c] [$mmol g^{-1}$]
MIL-101	3024	2.5	1.43	0
PMAP/MIL-101	564	2.3	0.27	0.34
PBSA/MIL-101	1107	2.3	0.52	1.01

[a] Pore size distribution is calculated based on the BJH model and desorption branch. [b] Total pore volume. [c] Active site is defined as either acidic or basic groups on the polymer, and the amount is determined on the basis of the loadings of polymer in the composites (see below).

reactants. Upon the filling of polymer, the pore diameter reduces by only 8%, from 2.5 nm to 2.3 nm. By contrast, the BET surface areas and pore volumes exhibit more significant decrease. In the dry state, there are strong intra- and inter-molecular interactions between polymer chains/segments. Therefore, the filled polymers form condense aggregation, which can potentially block the pore entre. This drastically reduces the N2 accessible surface area and volume. However, when the polymer-MIL-101 composites are used in solvent environment, the swelling of polymer can form large free volume to allow the diffusion of reactants. Furthermore, SEM and TEM experiments revealed that most of the vinyl monomers were polymerized inside the micropores of MIL-101 without bulk polymer formation on the external surface (see the Supporting Information, Figures S3 and S4). Thermogravimetric analysis (TGA; see the Supporting Information, Figure S5) confirmed the thermal stability of PBSA/MIL-101 and PMAP/MIL-101; the thermal decomposition temperature of the loaded polymer was higher (e.g., PBSA is ≈400 °C) than that of MIL-101 (≈350 °C). Powder X-ray diffraction (PXRD, Figure 3c) confirms the retention of the parent framework structure of octahedron-like morphology and the crystallinity of the resultant MOF-polymer composites.

Owing to the nature of linear, relatively short, and isolated polymeric chains within MOFs, the dissolution/swelling process would be facile because of the minimized polymer–polymer interaction. In addition, the dissolution process of the chiral polymeric chains is significantly easier than routine BSA-containing cross-linked PPBSA and MAP-containing cross-linked PPMAP resin (see the Supporting Information, Figure S6).

These functionalized acidic/basic polymers/MOF composites are used to catalyze one-pot tandem reactions (Table 2), which involve two steps: 1) deacetalization reaction by acid catalysis, and 2) Knoevenagel reaction by basic catalysis. It is notable that the linear PBSA and PMAP released from the alkaline digestion of the MIL-101 framework are completely soluble in the reaction solvent (DMSO/H_2O, 40:1, v/v), with a solubility of more than 20 mg mL^{-1} (see the Supporting Information, Figure S6). This further supports the coexistence of global heterogeneous and local homogenous domains in our designed catalytic system. We examined the model reaction of *p*-fluorobenzaldehyde glycol acetal and ethyl cyanoacetate in the presence of various heterogeneous and homogeneous catalysts. A mixture of a catalytic amount (5 mol%) of PBSA/MIL-101 and PMAP/MIL-101 (PBSA/MIL-101 + PMAP/MIL-101) efficiently catalyzed this reaction to give **4a** in a quantitative yield after 12 h (Table 2, entry 1), whereas a mixture of *p*-toluene sulfonic acid (PTSA) and 4-dimethylaminopyridine (MAP) as a homogeneous catalyst (5 mol%) showed no activity (entry 2), which is maybe due to the fast acid–base neutralization. In contrast, the use of a mixture of routine cross-linked polystyrene resins, PPBSA and PPMAP, only led to the deacetalization product **2a** in 33% yield. No formation of the desired product revealed that the exposure of incompatible catalytic sites on the surface of solid materials can remarkably interfere with each other upon mixing. Moreover, the addition of excessive amounts of free acid (TPSA, 5 equiv) or base (DMAP, 5 equiv) to the mixture of PBSA/MIL-101 and PMAP/MIL-101 can entirely stop the catalytic activity (entries 5 and 6), which demonstrates that the opening channel filled with catalytic sites can be readily reached by reaction substrate/opposite agents. This contrasting experiment can relate the catalytic performance to their structural features: the high porosity of PBSA/MIL-101 and PMAP/MIL-101 would provide sufficient guest-accessible room for catalysis. In addition, the unique structures of the MOF/chiral polymer composites that feature with heterogeneous matrix and local homogeneous active domain would contribute to the efficient catalytic site exposure of PBSA/MIL-101 and PMAP/MIL-101. The recyclability of the bifunctional catalyst (PBSA/MIL-101 + PMAP/MIL-101) is also excellent. The yield of the fourth run was about 83% of the value of the first run. After recycling, the crystallinity of the catalyst was maintained, as verified by PXRD (see the Supporting Information, Figure S7).

To demonstrate the versatility of these catalysts, we further extended the scope of this protocol to other aldehyde glycol acetals with cyanoacetate derivatives. As shown in Table 3, the electron-donating (OMe), electron-withdrawing (F), and neutral (R = H) groups at the *para* position of the benzene ring of aldehyde glycol acetal are all well tolerated to produce the expected products in good yields (entries 1–3). Furthermore, the size of the ester group (*i*Pr, *i*Bu, and *t*Bu) in the cyanoacetate showed only a slight influence on the reaction outcome (entries 4–6) to afford the desired products in moderate to good yields. Next, we turned our attention towards the bulk aldehyde glycol acetal **1d** as a substrate for this reaction, which is even larger than the window size of Cr-MIL-101. The expected product **4h** was only obtained in a trace amount (entry 7), which revealed that the catalytic reactions occur mostly in the cavities of the catalyst rather than on the external surface; thus, these heterogeneous catalysts exhibit reagent size selectivity.

Furthermore, bifunctional catalyst (PBSA/MIL-101 + PMAP/MIL-101) has also been evaluated in a tandem reaction that involves the hydrolysis of an acetal group followed by a Henry reaction (Scheme 1). Remarkably, the bifunctional catalytic composites can convert benzaldehyde glycol acetal **5** into the desired product **7** with a good yield of 94% without detection of any remaining aldehyde intermediate.

Table 2. One-pot sequential deacetalization/Knoevenagel reaction.[a]

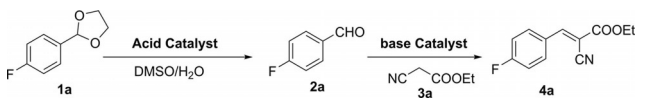

Entry	Catalyst	Conv. of **1a** [%][b]	Yield of **2a** [%][c]	Yield of **4a** [%][c]
1	PBSA/MIL-101 + PMAP/MIL-101	100	Trace	89
2	PTSA+DMAP	Trace	Trace	Trace
3	PPBSA+PPMAP	40	33	Trace
4	PBSA/MIL-101 + PMAP/MIL-101+DMAP	Trace	Trace	Trace
5	PBSA/MIL-101 + PMAP/MIL-101+PTSA	100	91	9

[a] Reaction conditions: **1a** (0.25 mmol), **3a** (0.3 mmol), DMSO/H_2O (40:1, *v/v*), 70 °C, 12 h. [b] Conversion of **1a** was determined by ^{1}H NMR spectroscopy of the crude reaction mixtures. [c] The yield was determined after isolation.

Table 3. A mixture of PBSA/MIL-101 and PMAP/MIL-101 catalyzed one-pot deacetalization/Knoevenagel reaction.[a]

Entry	1	3	Yield of 4 [%]
1	**1b**: R^1 = H	**3a**: R^2 = COOEt	**4b**: 93
2	**1c**: R^1 = OCH_3	**3a**: R^2 = COOEt	**4c**: 90
3	**1a**: R^1 = F	**3c**: R^2 = COOMe	**4d**: 86
4	**1a**: R^1 = F	**3d**: R^2 = COO*i*Pr	**4e**: 88
5	**1a**: R^1 = F	**3d**: R^2 = COO*i*Bu	**4f**: 78
6	**1a**: R^1 = F	**3d**: R^2 = COO*t*Bu	**4g**: 75
7	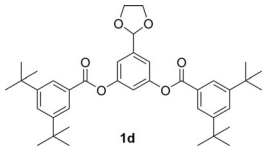	**3a**: R^2 = COOEt	**4h**: trace

[a] Reaction conditions: **1** (0.25 mmol), **3** (0.3 mmol), a mixture of PBSA/MIL-101 and PMAP/MIL-101 (5 mmol%, 0.0125 mmol), DMSO/H_2O (40:1, *v*/*v*), 70 °C, 12 h.

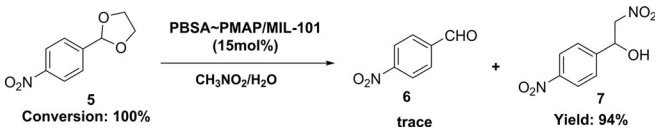

Scheme 1. A mixture of PBSA/MIL-101 and PMAP/MIL-101 catalyzed one-pot deacetalization/Henry reaction.

Conclusion

We have demonstrated the "wolf and lamb" concept with bifunctionlized linear polymer/MOF composites. The acidic and basic polymers were separately accommodated into the MOF by loading their corresponding monomers into the MOF cavities, and subsequently, carrying out the polymerization. These two types of polymer/MOF catalysts that bear isolated active sites work together to catalyze one-pot tandem reactions. The tightly intertwined assembly of linear polymers within the MOF architecture ensured that this heterogeneous material has good recyclability and provides excellent compartmentalization to spatially isolate incompatible or opposing reagents. More importantly, by contrast to the previous strategies to realize site-isolated catalysts, the polymer/MOF composite provides a unique local homogeneous and global heterogeneous microdomain.

Experimental Section

Chemicals and instrument information

NMR spectra were recorded on a Brüker DPX-400 or 500 spectrometer at 400 or 500 MHz and at 100 or 125 MHz for ^{1}H and ^{13}C NMR, respectively. Data for ^{1}H NMR were recorded as follows: chemical shift (δ = ppm), multiplicity (s, singlet; d, doublet; t, triplet; q, quartet; m, multiplet), coupling constant (J = Hz), integration. Data for ^{13}C NMR were reported in terms of chemical shift (δ = ppm). Mass spectra were determined on an Esquire-LC-00075 mass spectrometer. Infrared experiments were performed on a Brüker Alpha FTIR spectrometer by using a 1.0 mg sample of the solid at a 4 cm^{-1} resolution. PXRD data were collected at ambient temperature on a Bruker D8 Advance diffractometer at 40 kV and 40 mA for $Cu_{K\alpha}$ (λ = 1.5418 Å) with a scan speed of 1 sec/step, a step size of 0.02°, and a 2θ range of 5–40°. The Brunauer–Emmer–Teller (BET) surface areas were measured by using a Micromeritics ASAP 2020 analyzer at 77 K. TGA data were collected on a PerkinElmer TGA 7 Analyzer, which was run from 50 to 500 °C with a scan rate of 10 °C min^{-1}. Analyses of the morphology and chemical composition of the samples were conducted by using a Hitachi S-4800 field-emission scanning electron microscope (FE-SEM). The computational modeling for the topological characteristic of the host, monomers, and linear polymers was carried out on Discovery Studio 2.5 (Accelrys Software Inc., San Diego, CA). Gel permeation chromatography (GPC) analysis was performed by using a Waters 1525 pump with a refractive index (RI) detector. Starting materials and solvents were purchased from commercial suppliers (Sigma–Aldrich, Alfa Aesar, TCI, and others) and used without further.

The synthesis of the PBSA/MIL-101 composites

A solution of sodium 4-styrenesulfonate (300 mg, 1.46 mmol) and 2,2-azobisisobutyronitrile (AIBN, 45 mg, 0.27 mmol, as radical initiator) in DMF/H_2O (1.5 mL, 5:1, v/v) was impregnated into Cr-MIL-101 (0.7 g). The mixture was ground in a mortar and allowed to stand at 4 °C for 12 h to ensure the distribution equilibrium of the monomers through the cavities of MIL-101 was reached. The polymerization was conducted under a nitrogen atmosphere at 80 °C for 5 days. The resultant powder was soaked in DMF for 3 days and intensively washed with DMF to completely remove all unreacted monomer and loosely attached polymers. The residual DMF was removed by soaking and washing with acetone. Finally, the obtained composite was acidified by soaking in HCl (12 N) for 12 h followed by filtration and drying at 80 °C overnight.

The synthesis of the PMAP/MIL-101 composites

A solution of compound **S1** (300 mg, 1.34 mmol, see the Supporting Information) and 2,2-azobisisobutyronitrile (AIBN, 45 mg, 0.27 mmol), as a radical initiator, in toluene (1.5 mL) was impregnated into Cr-MIL-101 (0.7 g). The mixture was ground finely in a mortar and allowed to stand at 4 °C for 12 h to ensure the distribution equilibrium of the monomers through the cavities of MIL-101 was reached. The polymerization was conducted under a nitrogen atmosphere at 80 °C for 5 days. The resultant powder was soaked in DMF for 3 days and washed with acetone to remove the residual DMF. The powder was repeatedly washed with HCl (1 N) to completely remove all unreacted monomer and loosely attached polymers between MIL-101 particles. After the residue was soaked in 5% $NaHCO_3$ for 12 hours, the desired polymer composite PMAP/MIL-101 was obtained and further dried at 80 °C overnight.

The extraction of the linear polymer PBSA (or PMAP) from the PBSA/MIL-101 (or PMAP/MIL-101) composites for NMR and GPC analyses

PBSA/MIL-101 (200 mg) was first fully digested by NaOH (10 wt.%) at 120 °C for 10 min. The pH of the obtained solution was adjusted to slightly lower than 7 by using HCl (6 N). The NaPBSA, together with terephthalic acid, was precipitated by adding an excess amount of acetone. The precipitate was collected by filtration and

washed with diethyl ether to remove the terephthalic acid; however, pure NaPBSA polymer was not obtained, even after intensive washing. Nevertheless, the precipitate was dried and soaked in H_2O (2 mL). The insoluble solid was removed by filtration, and the filtrate was dried in vacuo. The resulting white solid was further dried in vacuo by using an oil pump at 120 °C for 4 h to afford the encapsulated PBSA. ^{1}H NMR (500 MHz, D_2O): $\delta = 7.83$ (d, $J = 7.8$ Hz, 2H), 6.78 (s, 2H), 2.68–1.04 ppm (m, 3H).

PMAP/MIL-101 (200 mg) was first fully digested by NaOH (10 wt.%) at 120 °C for 10 min. The precipitate was collected by filtration and fully dried. Then, the precipitate was soaked in CH_2Cl_2 (10 mL). The insoluble solid was removed by filtration, and the filtrate was dried in vacuo. The resulting solid was further dried in vacuo by using an oil pump at 120 °C for 4 h to afford the encapsulated PMAP. ^{1}H NMR (500 MHz, $CDCl_3$): $\delta = 8.11$ (s, 2H), 7.16–6.10 (m, 6H), 4.59–4.10 (m, 2H), 3.04 (m, 3H), 2.07–0.64 ppm (m, 4H).

Qualification for the PBSA loading amount with a unit of mmol g^{-1} in the PBSA/MIL-101 composite

Elemental analysis gave the value of *S* weight ratio in PBSA/MIL-101. *S* can only be derived from PBSA within a MOF. The molecular formula of PBSA is well defined (W_{PBSA}, $-(C_8H_8O_3S)_n-$); therefore, if we know the *S* weight content (W_s, %), the PBSA loading amount (*C*, mmol g^{-1}) in PBSA/MIL-101 composite can be calculated based on Equation (1):

$$C = \frac{\frac{W_s}{32*100} * W_{PBSA} * 1000}{W_{PBSA}} \quad (1)$$

Qualification for the PMAP loading amount with a unit of mmol g^{-1} in the PMAP/MIL-101 composite

PMAP/MIL-101 (2 g) was first fully digested by NaOH (10 wt.%) at 120 °C for 10 min. The precipitate was collected by filtration and fully dried. Then, the precipitate was extracted with CH_2Cl_2 (50 mL × 3). The organic phases were combined and dried in vacuo. The ^{1}H NMR analysis was performed by using dibromomethane (CH_2Br_2) as the internal standard (174 mg, 1 mmol). The molecular formula of PBSA is well defined (W_{PBSA}, $-(C_{15}H_{16}N_2)_n-$), Indeed, NMR analysis gave the value of PMAP/CH_2Br_2 molar ratio, which can be calculated by the ratio of the integral area between δ_{PMAP} (IA_{PMAP}, $\approx$4.9 ppm) and $\delta_{CH_2Br_2}$ ($IA_{CH_2Br_2}$, $\approx$5.5 ppm). Therefore, the PMAP loading amount (*C*, mmol g^{-1}) can be calculated by using Equation (2):

$$C = \frac{IA_{PMAP} / IA_{CH2Br2} * 1 * W_{PMAP}}{W_{PMAP} * 2} \quad (2)$$

Typical reaction procedure for the one-pot deacetalization/Knoevenagel reaction

A suspension of PBSA/MIL-101 (12.3 mg, 0.0125 mmol) and PMAP/MIL-101 (36.7 mg, 0.0125 mmol) in DMSO/H_2O (1 mL, 40:1, v/v) was stirred at room temperature for 1 h. The corresponding benzaldehyde glycol acetal (0.25 mmol) and cyanoacetate derivative (0.3 mmol) were added, and the mixture was heated to 70 °C for 6 h. The mixture was filtered, and the filter cake was washed with ethyl acetate. The organic phases were collected, dried over anhydrous Na_2SO_4, and concentrated in vacuo to obtain the crude product, which was purified by column chromatography (petroleum ether/ethyl acetate) to afford the pure product.

The reaction procedure for the one-pot deacetalization/Henry reaction

A suspension of PBSA/MIL-101 (37.1 mg, 0.0125 mmol) and PMAP/MIL-101 (110.3 mg, 0.0125 mmol) in nitromethane/H_2O (1 mL, 40:1 v/v) was stirred at room temperature for 1 h. 2-(4-nitrophenyl)-1,3-dioxolane (0.25 mmol) was added, and the mixture was heated to 70 °C for 6 h. The mixture was filtered and washed with methanol several times. The filtrates were combined, concentrated under vacuo, and purified by column chromatography (petroleum ether/ethyl acetate) to afford the pure product.

Acknowledgements

The authors gratefully acknowledge Prof. Chi-Ming Che at The Hong Kong University for their knowledge sharing and suggestions on Homogenization of Heterogeneous composites as catalytic system. Financial support from the National Natural Science Foundation of China (Nos. 21572096, 51603046), the National Key Basic Research Program of China (973 Program 2013CB834802), Shenzhen overseas high level talents innovation plan of technical innovation project (KQCX20150331101823702), Shenzhen special funds for the development of biomedicine, Internet, new energy, and new material industries (JCYJ20150430160022517) and South University of Science and Technology of China (FRG-SUSTC1501A-16) is greatly appreciated.

Conflict of interest

The authors declare no conflict of interest.

Keywords: hybrid catalysts · polymerization · polymers · metal–organic frameworks · tandem reaction

[1] a) S. F. Mayer, W. Kroutil, K. Faber, *Chem. Soc. Rev.* **2001**, *30*, 332; b) R. N. Perham, *Annu. Rev. Biochem.* **2000**, *69*, 961–1004; c) T. Nakayama, H. Suzuki, T. Nishino, *J. Mol. Catal. B* **2003**, *23*, 117; d) D. Arigoni, S. Sagner, C. Latzel, W. Eisenreich, A. Bacher, M. H. Zenk, *Proc. Natl. Acad. Sci. USA* **1997**, *94*, 10600; e) C. M. Agapakis, P. M. Boyle, P. A. Silver, *Nat. Chem. Biol.* **2012**, *8*, 527.

[2] a) L. F. Tietze, *Chem. Rev.* **1996**, *96*, 115–136; b) H. Pellissier, *Chem. Rev.* **2013**, *113*, 442–524.

[3] B. J. Cohen, M. A. Kraus, A. Patchornik, *J. Am. Chem. Soc.* **1981**, *103*, 7620.

[4] a) H. Huang, C. A. Denard, R. Alamillo, A. J. Crisci, Y. Miao, J. A. Dumesic, S. L. Scott, H. Zhao, *ACS Catal.* **2014**, *4*, 2165; b) Z. J. Wang, K. N. Clary, R. G. Bergman, K. N. Raymond, F. D. Toste, *Nat. Chem.* **2013**, *5*, 100; c) Y. Yang, X. Liu, X. Li, J. Zhao, S. Bai, J. Liu, Q. Yang, *Angew. Chem. Int. Ed.* **2012**, *51*, 9164; *Angew. Chem.* **2012**, *124*, 9298; d) R. J. R. W. Peters, I. Louzao, J. C. M. van Hest, *Chem. Sci.* **2012**, *3*, 335; e) J. Shi, L. Zhang, Z. Jiang, *ACS Appl. Mater. Interfaces* **2011**, *3*, 881; f) M. B. Runge, M. T. Mwangi, A. L. Miller II, M. Perring, N. B. Bowden, *Angew. Chem. Int. Ed.* **2008**, *47*, 935; *Angew. Chem.* **2008**, *120*, 949; g) A. L. Miller II, N. B. Bowden, *Adv. Mater.* **2008**, *20*, 4195–4199; h) A. W. Pilling, J. Boehmer, D. J. Dixon, *Angew. Chem. Int. Ed.* **2007**, *46*, 5428; *Angew. Chem.* **2007**, *119*, 5524; i) S. L. Poe, M. Kobašlija, D. T. McQuade, *J. Am. Chem. Soc.* **2006**, *128*, 15586; j) N. T. S. Phan, C. S. Gill, J. V. Nguyen, Z. J. Zhang, C. W. Jones, *Angew. Chem. Int. Ed.* **2006**, *45*, 2209; *Angew. Chem.* **2006**, *118*, 2267; k) B. Helms, S. J. Guillaudeu, Y. Xie, M. McMurdo, C. J. Hawker, J. M. J. Fréchet, *Angew. Chem. Int. Ed.* **2005**, *44*, 6384; *Angew. Chem.* **2005**, *117*, 6542.

[5] a) F. Gelman, J. Blum, D. Avnir, *J. Am. Chem. Soc.* **2002**, *124*, 14460; b) F. Gelman, J. Blum, D. Avnir, *Angew. Chem. Int. Ed.* **2001**, *40*, 3647; *Angew. Chem.* **2001**, *113*, 3759; c) F. Gelman, J. Blum, D. Avnir, *J. Am. Chem. Soc.* **2000**, *122*, 11999.

[6] H. Yang, L. Fu, L. Wei, J. Liang, B. P. Binks, *J. Am. Chem. Soc.* **2015**, *137*, 1362.

[7] a) Y. Chi, S. T. Scroggins, J. M. J. Fréchet, *J. Am. Chem. Soc.* **2008**, *130*, 6322; b) J. Lu, J. Dimroth, M. Weck, *J. Am. Chem. Soc.* **2015**, *137*, 12984;c) L. Xiong, H. Zhang, A. Zhong, Z. He, K. Huang, *Chem. Commun.* **2014**, *50*, 14778.

[8] a) M. P. Suh, H. J. Park, T. K. Prasad, D. W. Lim, *Chem. Rev.* **2012**, *112*, 782; b) K. Sumida, D. L. Rogow, J. A. Mason, T. M. McDonald, E. D. Bloch, Z. R. Herm, T. H. Bae, J. R. Long, *Chem. Rev.* **2012**, *112*, 724; c) J. R. Li, J. Sculley, H. C. Zhou, *Chem. Rev.* **2012**, *112*, 869; d) P. Horcajada, R. Gref, T. Baati, P. K. Allan, G. Maurin, P. Couvreur, G. Ferey, R. E. Morris, C. Serre, *Chem. Rev.* **2012**, *112*, 1232; e) J. Lee, O. K. Farha, J. Roberts, K. A. Scheidt, S. T. Nguyen, J. T. Hupp, *Chem. Soc. Rev.* **2009**, *38*, 1450; f) Q. Yang, Q. Xu, H. L. Jiang, *Chem. Soc. Rev.* **2017**, *46*, 4774 – 4808; g) L. Zhu, X. Q. Liu, H. L. Jiang, L. B. Sun, *Chem. Rev.* **2017**, *117*, 8129 – 8176;h) Y. Jiang, X. Zhang, X. Dai, W. Zhang, Q. Sheng, H. Zhuo, Y. Xiao, H. Wang, *Nano Res.* **2017**, *10*, 876; i) C. Hou, G. Zhao, Y. Ji, Z. Niu, D. Wang, Y. Li, *Nano Res.* **2014**, *7*, 1364; j) H. Wu, C. Shen, C. Xia, L. He, *Sci. China Mater.* **2017**, *60*, 1269; k) Y. Pan, B. Yuan, Y. Li, D. He, *Chem. Commun.* **2010**, *46*, 2280; l) F. Vermoortele, R. Ameloot, A. Vimont, C. Serre, D. Devos, *Chem. Commun.* **2011**, *47*, 1521; m) L. M. Aguirre-Díaz, F. Gándara, M. Iglesias, N. Snejko, E. Gutiérrez-Puebla, M. Á. Monge, *J. Am. Chem. Soc.* **2015**, *137*, 6132.

[9] a) G. Distefano, H. Suzuki, M. Tsujimoto, S. Isoda, S. Bracco, A. Comotti, P. Sozzani, T. Uemura, S. Kitagawa, *Nat. Chem.* **2013**, *5*, 335; b) T. Uemura, Y. Ono, Y. Hijikata, S. Kitagawa, *J. Am. Chem. Soc.* **2010**, *132*, 4917; c) T. Uemura, N. Uchida, A. Asano, A. Saeki, S. Seki, M. Tsujimoto, S. Isoda, S. Kitagawa, *J. Am. Chem. Soc.* **2012**, *134*, 8360; d) G. Distefano, A. Comotti, S. Bracco, M. Beretta, P. Sozzani, *Angew. Chem. Int. Ed.* **2012**, *51*, 9258; *Angew. Chem.* **2012**, *124*, 9392.

[10] a) L. Gao, C. Y. Li, K. Y. Chan, Z. N. Chen, *J. Am. Chem. Soc.* **2014**, *136*, 7209; b) L. Bromberg, X. Su, T. A. Hatton, *Chem. Mater.* **2014**, *26*, 6257; c) Z. Zhang, H. T. H. Nguyen, S. A. Miller, S. M. Cohen, *Angew. Chem. Int. Ed.* **2015**, *54*, 6152; *Angew. Chem.* **2015**, *127*, 6250.

[11] a) X.-W. Dong, T. Liu, Y.-Z. Hu, X.-Y. Liu, C.-M. Che, *Chem. Commun.* **2013**, *49*, 7681; b) T. Liu, J.-X. Che, Y.-Z. Hu, X.-W. Dong, X.-Y. Liu, C.-M. Che, *Chem. Eur. J.* **2014**, *20*, 14090; c) T. Liu, D.-Q. Li, S.-Y. Wang, Y.-Z. Hu, X.-W. Dong, X.-Y. Liu, C.-M. Che, *Chem. Commun.* **2014**, *50*, 13261.

[12] G. Ferey, C. Mellot-Draznieks, C. Serre, F. Millange, J. Dutour, S. Surble, I. Margiolaki, *Science* **2005**, *309*, 2040.

[13] M. F. De Lange, J.-J. Gutierrez-Sevillano, S. Hamad, T. J. H. Vlugt, S. Calero, J. Gascon, F. Kapteihn, *J. Phys. Chem. C* **2013**, *117*, 7613 – 7622.

Manuscript received: March 20, 2018

Accepted manuscript online: April 25, 2018

Version of record online: June 19, 2018